C94/09/12.1

CMU-HEP94-34

For the Proceedings of the XXIV International Symposium on Multiparticle Dynamics, Eds. A. Giovannini, S. Lupia and R. Ugoccioni, World Scientific, Singapore.

Fermilab Library 0 1160 0054284 9

CMU-HEP-94-34

A New Phenomenological Model for Strange Baryon Production in Hadronic Interactions

Erik Gottschalk

Department of Physics
Carnegie Mellon University
Pittsburgh, Pennsylvania 15213, USA

(representing the BNL E766 Collaboration)

FERMILAB
DEC 7 199
LIBRARY

ABSTRACT

A new phenomenological model for hadronic production of strange baryons is presented. The model was developed using fully reconstructed events belonging to topologies with a single strange baryon produced in 27.5 GeV/c proton-proton interactions. Low multiplicity topologies are dominated by single diffraction dissociation reactions, whereas high multiplicity topologies display little evidence for diffractive production processes.

1. Overview

Models continue to be an important tool in the study of hadron-hadron interactions. Hadronic interactions encompass a range of complex processes that are responsible for the production of many kinds of particles in enormous numbers of different states. In many analyses, ranging from studies of specific particles to studies of general features of multiparticle final states, the only tools that are available to help unravel the complexity of the underlying hadronic interactions are models. The development of new models and the refinement of older models is an important aspect of the current research being done in particle physics.

We have developed a simple phenomenological model for strange baryon production based on an analysis of a large—2 million event—sample of fully reconstructed events (events in which all particles were measured and identified). This data sample was obtained by experiment E766 at Brookhaven National Laboratory (BNL). A multiparticle spectrometer (shown in Figure 1) was used to study proton-proton interactions at an energy of $\sqrt{s}$ = 7.3 GeV. Using a multiplicity trigger to select high multiplicity events, we collected a sample of 3 x 10^8 events with an average of nine charged tracks. In our analysis of the production of strange baryons (Λ, Ξ^-, and Ω^-), we studied features of *pp* interactions that produced a single strange baryon in multiparticle final states with multiplicities ranging from 6 to 14 charged particles. Our model was developed to reproduce these multiparticle final states in their entirety.

The data analysis, which is described elsewhere[1], entailed track reconstruction for events with multiplicities as high as 20 charged particles. Strange baryons were found by using these reconstructed trajectories to reconstruct decay vertices. The final stage in the analysis that led to complete event reconstruction used direct particle identification, based on Cherenkov and time-of-flight measurements, and indirect particle identification.

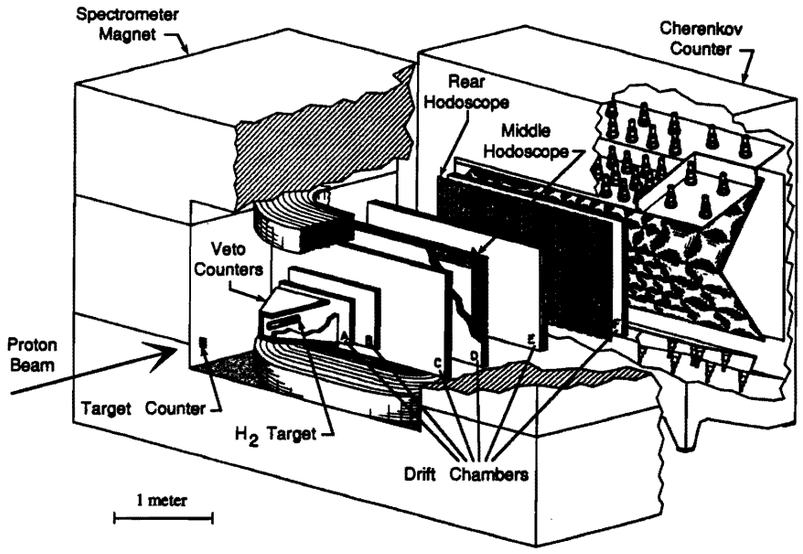

Figure 1: The BNL E766 Multiparticle Spectrometer.

Indirect particle identification was based on applying kinematic constraints (energy and momentum conservation) and conserved quantities (electric charge, baryon number, and strangeness) to fully reconstruct events. Fully reconstructed events were categorized by assigning events to specific final state topologies, and topologies with a single strange baryon were subsequently selected for our study of strange baryon production[2].

In this paper we present results on Λ production. We discuss five reactions of the type $p\,p \rightarrow p\,\Lambda\,K^+\,(\pi^+\,\pi^-)^n$, where n = 1, 2, 3, 4, 5 and the Λ decays to $p\,\pi^-$. Low multiplicity topologies (n = 1, 2) are dominated by single diffraction dissociation reactions[3], whereas high multiplicity topologies (n = 4, 5) display little evidence for diffractive production processes. Our model for Λ production reproduces these and other features of the data.

2. Phenomenological Model for Λ Production

As yet there is no fundamental theory that can be used to calculate the distribution of particles produced in hadronic interactions. Furthermore, the Monte Carlo models most often used in high energy physics analyses do not reproduce all of the features of low p_t events, which represent both the bulk of hadronic cross sections and an important source of the background of higher mass, higher p_t phenomena. For example, we compared our data for a particular topology to events generated by PYTHIA[4] version 5.6. We generated minimum-bias pp events with $\sqrt{s}$ = 7.3 GeV and then selected $p\,p \rightarrow p\,(\Lambda\,K^+\,\pi^+\,\pi^-)$ events for comparison to real events. The reason we selected this particular topology is that it has one of the largest cross sections for Λ production in our data. To compare the PYTHIA events to data we looked at M_X^2 distributions, where M_X^2 was

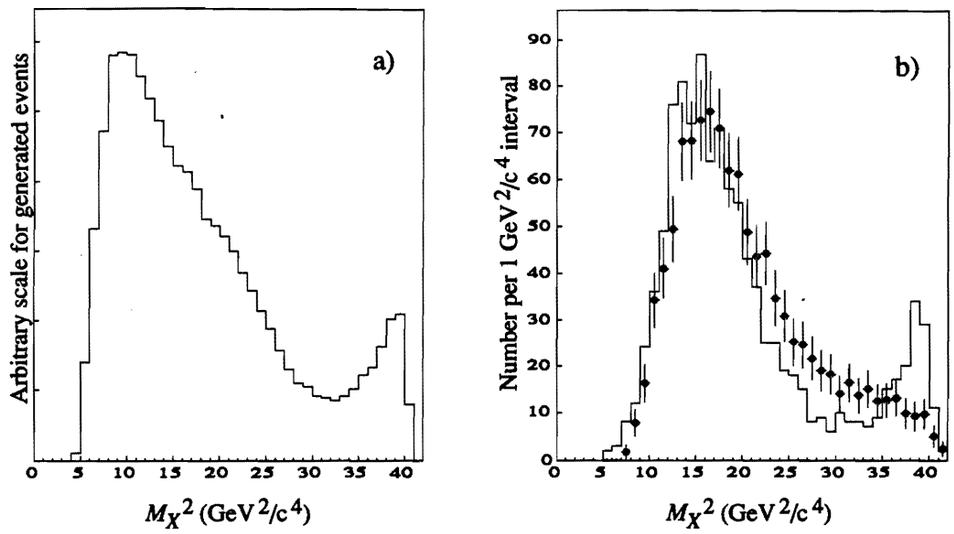

Figure 2: $M_X{}^2$ for (a) $p\,p \rightarrow p\,(\Lambda\,K^+\,\pi^+\,\pi^-)$ events generated by PYTHIA, and for (b) PYTHIA events after the events were passed through a software simulation of the detector (solid line) compared to $M_X{}^2$ for the data (data points with error bars).

defined to be the invariant mass squared of all final state particles excluding the proton. Figure 2(a) shows $M_X{}^2$ for events generated by PYTHIA, and Figure 2(b) shows the $M_X{}^2$ distribution for PYTHIA events (solid line) after the events have passed through a software simulation of our detector. The data, which are shown as data points with error bars in Figure 2(b), do not display the peak that is seen for PYTHIA events near the kinematic limit for $M_X{}^2$ (for a 27.5 GeV/c beam proton the kinematic limit for $M_X{}^2$ is 40.6 GeV^2/c^4). Qualitative differences such as this can be significant, especially when the primary interest in a given "soft" reaction is as a background to a "hard" process.

Two of the most important features of the data are observed in $M_X{}^2$ distributions for the five $p\,p \rightarrow p\,\Lambda\,K^+\,(\pi^+\,\pi^-)^n$ topologies. The low multiplicity topologies, which have one or two pion pairs, display a low mass enhancement in $M_X{}^2$. This means that the final state proton is isolated from all other final state particles—a feature that is characteristic of single diffraction dissociation reactions. High multiplicity topologies, which have four or five pion pairs, have $M_X{}^2$ distributions that peak at the kinematic limit of $M_X{}^2$; the proton is no longer isolated from other particles.

These two features of the data are represented by two components, referred to as Model A and Model B, in our phenomenological model for Λ production. Model A reproduces features of the data observed in low multiplicity events, while Model B is used for high multiplicity events. For intermediate multiplicities we combine these two components of the model to reproduce the data.

Both Model A and Model B generate events as $p\,p \rightarrow p\,X$ (see Table 1). The two-body $p\,X$ system is generated by specifying $M_X{}^2$ and proton $p_t{}^2$, which is the square of the proton's transverse momentum with respect to the beam direction. The breakup of the X system into $\Lambda\,K^+\,(\pi^+\,\pi^-)^n$ is modeled by using a p_t-limited phase space generator

Table 1: Phenomenological model for topologies $p\,p \rightarrow p\,\Lambda\,K^+\,(\pi^+\,\pi^-)^n$, where $n = 1, 2, 3, 4, 5$.

Model A ($pp \rightarrow pX$)	Model B ($pp \rightarrow pX$)
M_X^2 rises to a peak and falls with a $dN/dM_X^2 \sim 1/M_X^6$ distribution	M_X^2 rises to a flat plateau with a $dN/dM_X^2 \sim M_X^{12}$ distribution
Proton p_t^2: $dN/dp_t^2 \sim e^{-4p_t^2}$	Proton p_t^2: $dN/dp_t^2 \sim e^{-2p_t^2}$
p_t-limited phase space: $f_A(S_{GJ})$	p_t-limited phase space: $f_B(S_{GJ})$
Longitudinal momentum of Λ modified to reproduce leading particle effect	

that includes a parameter to reproduce the leading particle effect that we observe for the Λ momentum distribution in the data. The only other parameter that is required to reproduce the data is the relative fraction of Model A and Model B. For the lowest multiplicity topology we use only Model A. For $n = 4$ and $n = 5$, only Model B is used. For $n = 2$, we use 60% Model A and 40% Model B, while for $n = 3$ the ratio is 40% Model A and 60% Model B.

3. Comparisons to Data

Events generated by our model are in good agreement with real events observed in the data. Since our events are fully reconstructed, we can compare any imaginable type of observed single- or multi-particle distribution to the model. All of the histograms presented in this section have the same format. For example, Figure 3 shows M_X^2 distributions for the five $p\,p \rightarrow p\,\Lambda\,K^+\,(\pi^+\,\pi^-)^n$ topologies: distributions for generated events are shown in the left column of histograms and to the right are distributions for generated events that have passed through a software simulation of our detector (solid line) together with the data (data points with error bars). All of the distributions in Figures 3 thru 7 are shown for events with final state proton $p_z < 0$ (p_z is the longitudinal momentum with respect to the beam in the center-of-mass frame).

Figure 3 shows M_X^2 and proton p_t^2 distributions. Since both of these distributions are parameterized in the model (see Table 1), any disagreements between the generated events and the data pinpoint improvements that could be made for a particular event generator. For example, for the topology with $n = 3$ pion pairs the M_X^2 distribution for Model B must be shifted to a higher value of M_X^2 to achieve good agreement between generated events and the data.

For the two lowest multiplicity topologies ($n = 1, 2$), Figure 3 shows a dotted line that suggests what the M_X^2 distribution might look like in the low M_X^2 region where our detector had no acceptance for events belonging to these particular topologies. The figure also has arrows that mark the threshold value for M_X^2 for each topology, and the

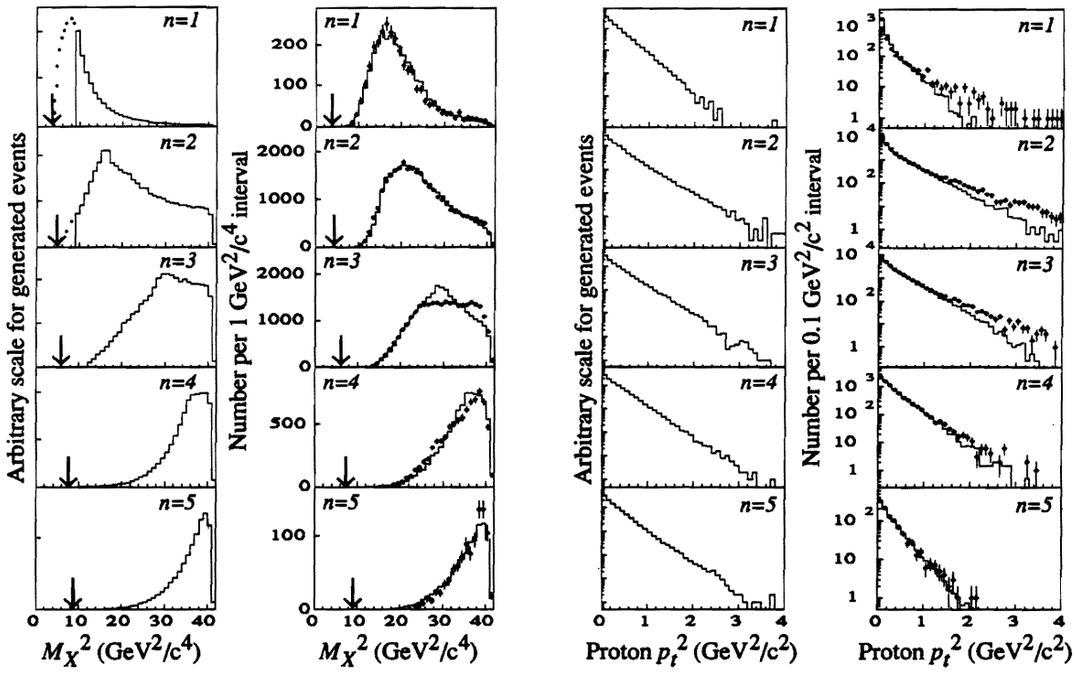

Figure 3: $M_X{}^2$ and proton $p_t{}^2$ distributions for $p\,p \rightarrow p\,\Lambda\,K^+\,(\pi^+\,\pi^-)^n$ topologies.

histograms show the dramatic shift from the low mass enhancement for low multiplicity events to peaking at the kinematic limit for $M_X{}^2$ for high multiplicity events.

Histograms in figures 4 and 5 show good agreement between generated events and the data for p_z and $p_t{}^2$ distributions in the center-of-mass frame for all final state particles excluding the proton. Except for Λ p_z distributions, none of the generated distributions in these figures are input to our model. The Λ p_z distributions are included in the model to reproduce the tendency of the Λ to be produced in the opposite hemisphere of the final state proton. This leading particle effect diminishes as the multiplicity increases.

Two-particle invariant mass distributions are shown in Figures 6 and 7. The differences between generated events and the data are due to hadronic resonances, which are not included in our model. There is ample evidence in the data for $\Delta(1232)^{++} \rightarrow p\pi^+$, $\Sigma(1385)^+ \rightarrow \Lambda\pi^+$, $\Sigma(1385)^- \rightarrow \Lambda\pi^-$, $K^*(892) \rightarrow K^+\pi^-$, $K^*(1430) \rightarrow K^+\pi^-$, and $\rho(770) \rightarrow \pi^+\,\pi^-$; and some evidence for other resonances that do not stand out as clearly as those just mentioned. All of the invariant mass distributions are shown with equal numbers of generated events and real events from the data. The agreement between the data and the model is quite good in regions in which there are no obvious peaks for resonances.

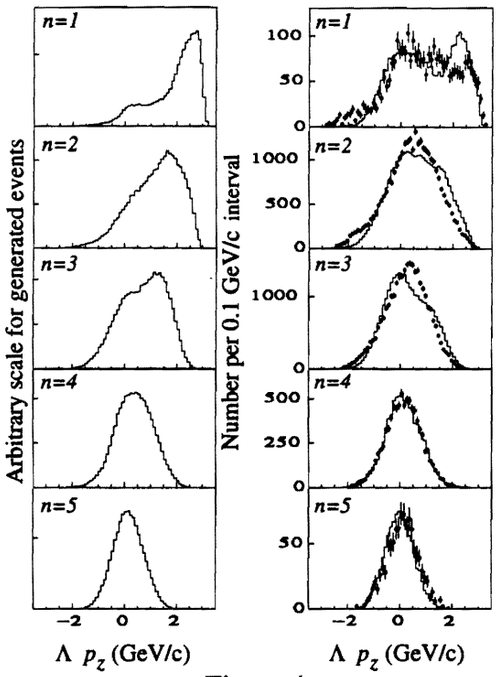

Figure 4a

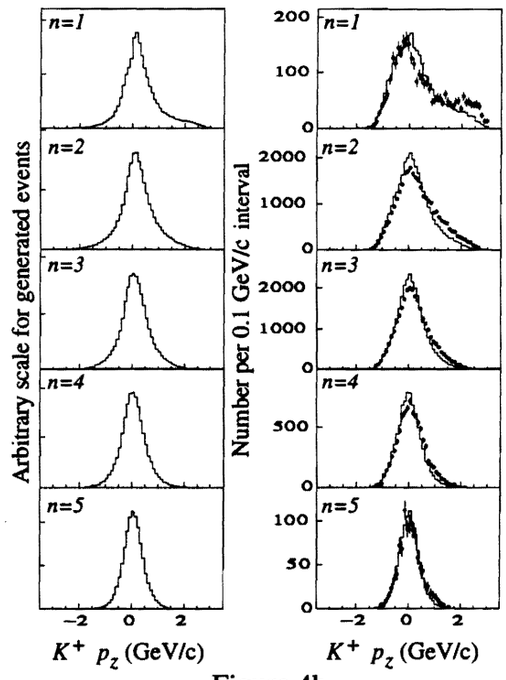

Figure 4b

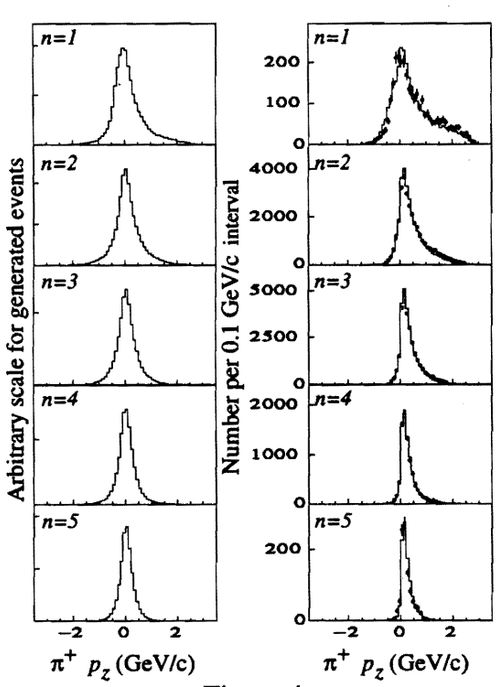

Figure 4c

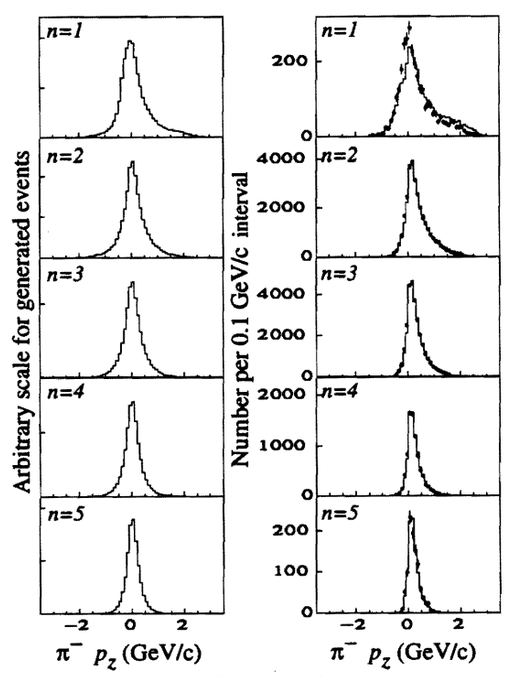

Figure 4d

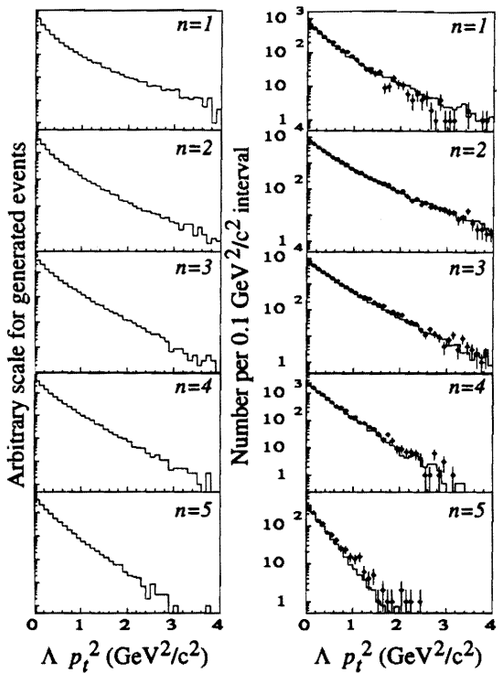

Figure 5a

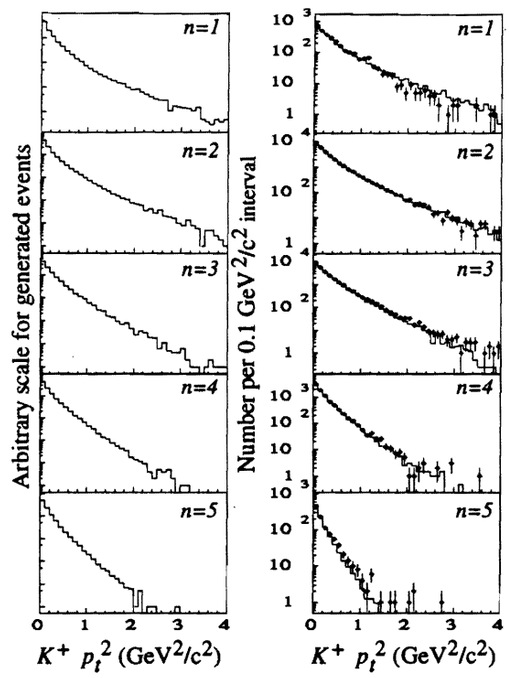

Figure 5b

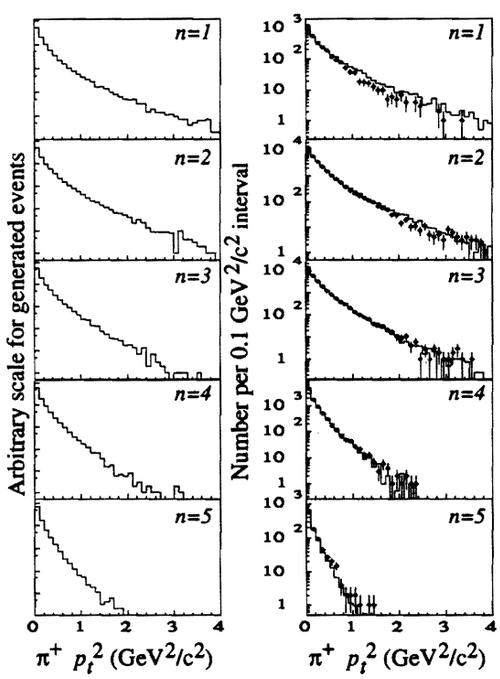

Figure 5c

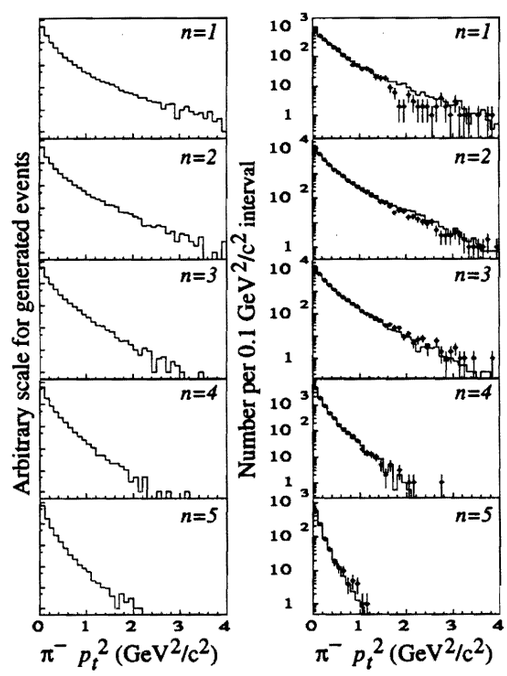

Figure 5d

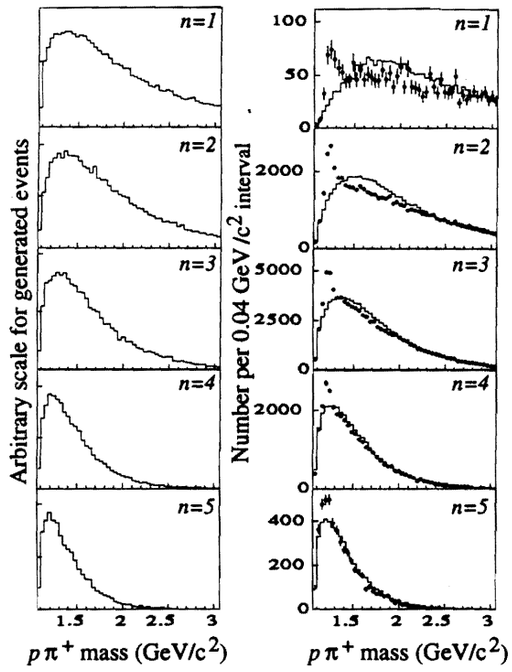

Figure 6a

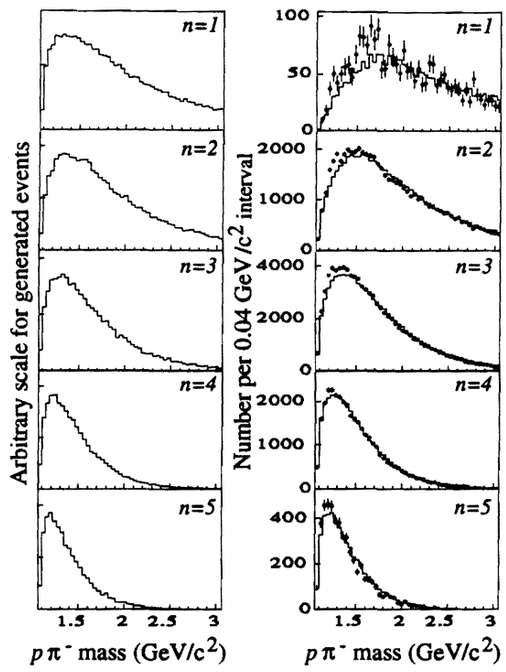

Figure 6b

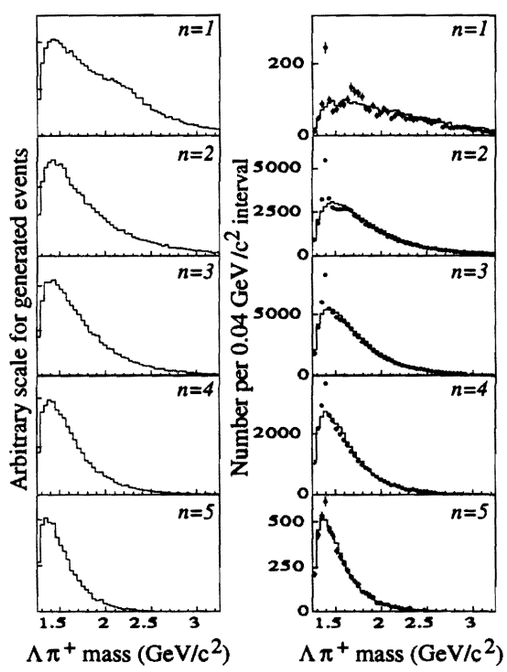

Figure 6c

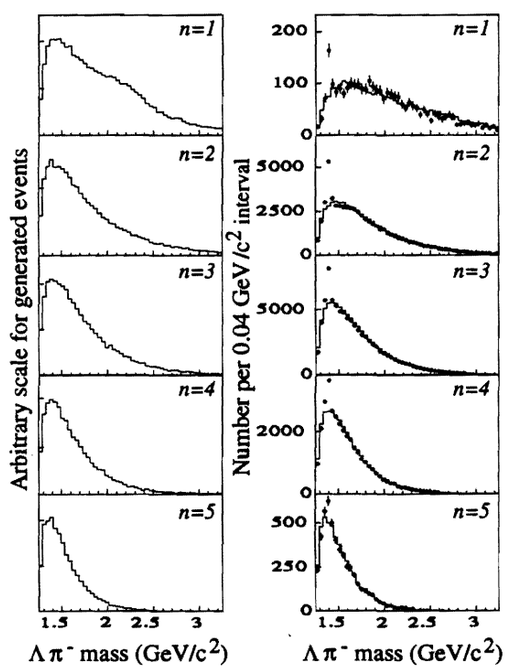

Figure 6d

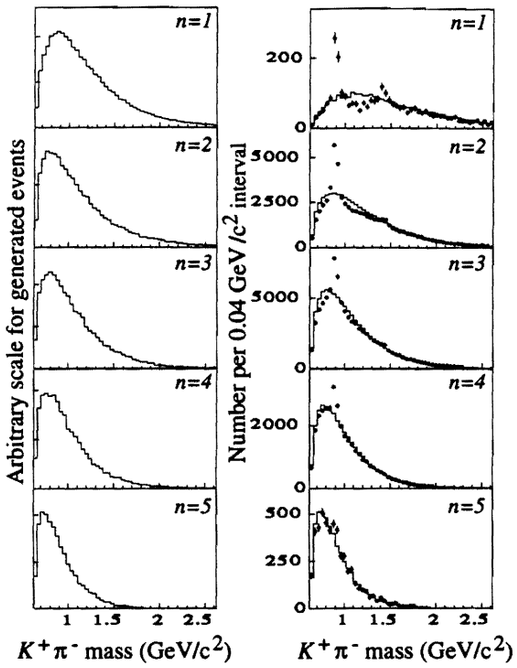

Figure 7a

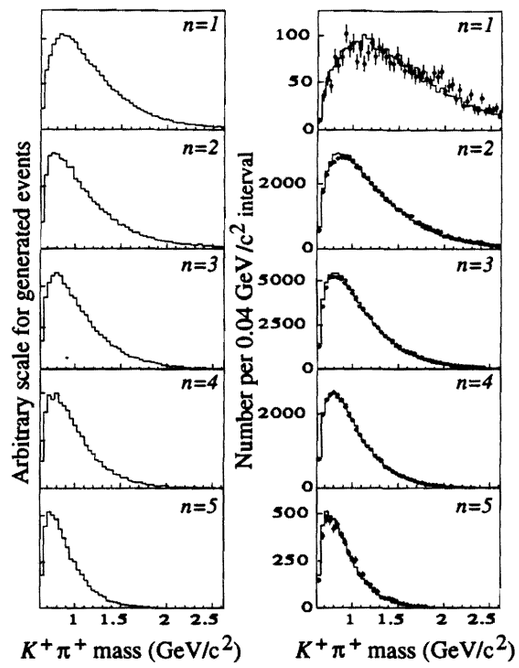

Figure 7b

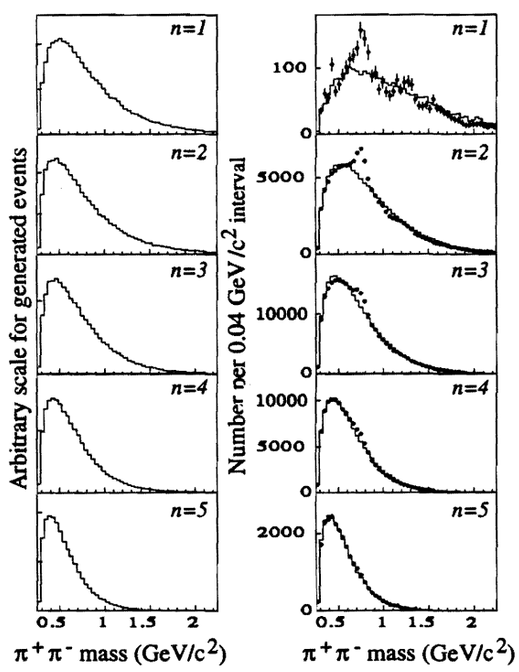

Figure 7c

4. Conclusions

Using fully reconstructed events belonging to the topologies $p\,p \rightarrow p\,\Lambda\,K^{+}\,(\pi^{+}\,\pi^{-})^{n}$ with n ranging from one to five, we have developed a new phenomenological model for the hadronic production of strange baryons. Although our model has been presented for a specific set of topologies, the model has been applied to Ξ^{-} production[5] and appears to be applicable to a range of topologies, not just topologies with single strange baryons.

The strengths of this model are its simplicity and its accurate reproduction of data belonging to topologies with a wide range of multiplicities. With only a few parameters, the model is able to reproduce the salient features of the data. In low multiplicity topologies we observe a pronounced low mass enhancement in M_X^2, the invariant mass squared of all final state particles excluding the proton, and a distinct tendency for the Λ to be produced in the opposite hemisphere of the final state proton. In high multiplicity topologies, on the other hand, the M_X^2 distributions peak at the kinematic limit of M_X^2, and the Λ no longer displays a leading particle effect; both the proton and the Λ have momentum distributions that look like the momentum distributions for other final state particles (K^{+}, π^{+}, and π^{-}). Our model has been designed to reproduce these features of the data. The model also reproduces other aspects of the data; such as the momentum distributions for individual particles in both low and high multiplicity topologies, and the nonresonant background in two-particle invariant mass distributions.

5. Acknowledgements

We acknowledge the assistance of the technical staffs at the AGS at Brookhaven National Laboratories, Columbia University Nevis Laboratories, Fermi National Accelerator Laboratory, and the University of Massachusetts. This work was funded in part by the National Science Foundation under Grants No. PHY90-14879 and PHY89-21320, by the Department of Energy Contracts No. DE-AC02-76CHO3000 and No. DE-AS05-87ER40356, and by CONACyT de Mexico.

6. References

1. J. Uribe et al., Phys. Rev. D **49**, 4373 (1994).
2. E.E. Gottschalk, "Strange Baryon Production in 27.5 GeV/c Proton-Proton Interactions", Ph.D. thesis, Columbia University (1992).
3. M.L. Good and W.D. Walker, Phys. Rev. **120**, 1857 (1960).
4. H.-U. Bengtsson and T. Sjöstrand, Computer Physics Commun. **46**, 43 (1987).
5. E.E. Gottschalk, pp. 70–72; and (in preparation).

CPHCB